

---

# Selectivity of $^{18}\text{F}$ -FLT and $^{18}\text{F}$ -FDG for Differentiating Tumor from Inflammation in a Rodent Model

Aren van Waarde, PhD<sup>1</sup>; David C.P. Cobben, MD<sup>1</sup>; Albert J.H. Suurmeijer, PhD<sup>2</sup>; Bram Maas<sup>1</sup>; Willem Vaalburg, PhD<sup>1</sup>; Erik F.J. de Vries, PhD<sup>1</sup>; Pieter L. Jager, PhD<sup>1</sup>; Harald J. Hoekstra, PhD<sup>3</sup>; and Philip H. Elsinga, PhD<sup>1</sup>

<sup>1</sup>PET Center, Groningen University Hospital, Groningen, The Netherlands; <sup>2</sup>Department of Pathology and Laboratory Medicine, Groningen University Hospital, Groningen, The Netherlands; and <sup>3</sup>Department of Surgical Oncology, Groningen University Hospital, Groningen, The Netherlands

---

Increased glucose metabolism of inflammatory tissues is the main source of false-positive  $^{18}\text{F}$ -FDG PET findings in oncology. It has been suggested that radiolabeled nucleosides might be more tumor specific. **Methods:** To test this hypothesis, we compared the biodistribution of 3'-deoxy-3'- $^{18}\text{F}$ -fluorothymidine (FLT) and  $^{18}\text{F}$ -FDG in Wistar rats that bore tumors (C6 rat glioma in the right shoulder) and also had sterile inflammation in the left calf muscle (induced by injection of 0.1 mL of turpentine). Twenty-four hours after turpentine injection, the rats received an intravenous bolus (30 MBq) of either  $^{18}\text{F}$ -FLT ( $n = 5$ ) or  $^{18}\text{F}$ -FDG ( $n = 5$ ). Pretreatment of the animals with thymidine phosphorylase ( $>1,000$  U/kg, intravenously) before injection of  $^{18}\text{F}$ -FLT proved to be necessary to reduce the serum levels of endogenous thymidine and achieve satisfactory tumor uptake of radioactivity. **Results:** Tumor-to-muscle ratios of  $^{18}\text{F}$ -FDG at 2 h after injection ( $13.2 \pm 3.0$ ) were higher than those of  $^{18}\text{F}$ -FLT ( $3.8 \pm 1.3$ ).  $^{18}\text{F}$ -FDG showed high physiologic uptake in brain and heart, whereas  $^{18}\text{F}$ -FLT was avidly taken up by bone marrow.  $^{18}\text{F}$ -FDG accumulated in the inflamed muscle, with  $4.8 \pm 1.2$  times higher uptake in the affected thigh than in the contralateral healthy thigh, in contrast to  $^{18}\text{F}$ -FLT, for which this ratio was not significantly different from unity ( $1.3 \pm 0.4$ ). **Conclusion:** In  $^{18}\text{F}$ -FDG PET images, both tumor and inflammation were visible, but  $^{18}\text{F}$ -FLT PET showed only the tumor. Thus, the hypothesis that  $^{18}\text{F}$ -FLT has a higher tumor specificity was confirmed in our animal model.

**J Nucl Med 2004; 45:695–700**

---

**F**DG labeled with  $^{18}\text{F}$  is currently the most widely used radiopharmaceutical in clinical oncology. This analog of glucose is trapped in tissues after phosphorylation by hexokinase but is not a substrate for glycolysis. Although the applications of  $^{18}\text{F}$ -FDG PET in tumor detection, staging,

and therapy evaluation are rapidly expanding,  $^{18}\text{F}$ -FDG uptake is not tumor specific. Various forms of inflammatory lesions also take up  $^{18}\text{F}$ -FDG and are a major cause of false-positive results. Histologic confirmation of  $^{18}\text{F}$ -FDG-positive lesions is therefore required for many types of tumors (1–6). Macrophages, which invade tumors, especially after anticancer therapy, can induce high  $^{18}\text{F}$ -FDG uptake as well and can complicate the interpretation of  $^{18}\text{F}$ -FDG PET images (1,7–9). Decreased uptake of  $^{18}\text{F}$ -FDG is seen in hyperglycemic patients and can cause false-negative results.

Another approach for tumor visualization is the use of radiolabeled nucleosides such as  $^{11}\text{C}$ -thymidine. Because  $^{11}\text{C}$ -thymidine is rapidly incorporated into newly synthesized DNA, this radiopharmaceutical can be used to image cellular proliferation. Animal and in vitro studies have suggested that thymidine uptake is considerable in malignant tissue but much less in inflammatory cells than is  $^{18}\text{F}$ -FDG uptake (10,11). Unfortunately, the imaging quality of  $^{11}\text{C}$ -thymidine is relatively poor, and its clinical applications are limited because of rapid in vivo degradation and the short half-life of  $^{11}\text{C}$  (20 min) (12–14).

However, the pyrimidine analog 3'-deoxy-3'-fluorothymidine (FLT) can be labeled with  $^{18}\text{F}$  (half-life, 109.8 min) and is resistant to metabolic breakdown (15).  $^{18}\text{F}$ -FLT is transported by the same nucleoside carrier as is thymidine and is also phosphorylated by the same enzyme, S-phase-specific thymidine kinase 1, which leads to intracellular trapping of radioactivity within the cytosol (16–21). In contrast to thymidine,  $^{18}\text{F}$ -FLT remains in the cytosolic fraction as  $^{18}\text{F}$ -FLT monophosphate and acts as a DNA chain terminator because of the 3' substitution (17). Thus, only a very slight DNA incorporation of  $^{18}\text{F}$ -FLT has been observed in cell lines (18).

Although inflammatory cells display a high metabolic activity and an avid uptake of  $^{18}\text{F}$ -FDG, they are recruited from elsewhere and do not divide at the site of inflammation. Because the mitotic activity of inflammatory cells is

---

Received Sep. 23, 2003; revision accepted Dec. 2, 2003.

For correspondence or reprints contact: Philip H. Elsinga, PET Center, Groningen University Hospital, P.O. Box 30001, 9700RB Groningen, The Netherlands.

E-mail: p.h.elsinga@pet.azg.nl

low, these cells can be expected to show a relatively low uptake of radiolabeled nucleosides. Thus,  $^{18}\text{F}$ -FLT may overcome a major drawback of  $^{18}\text{F}$ -FDG imaging.

To the best of our knowledge, no studies comparing the selectivity of  $^{18}\text{F}$ -FDG and  $^{18}\text{F}$ -FLT for tumor and inflammation have been reported in the literature. Therefore, we decided to examine the biodistribution of these radiopharmaceuticals in male Wistar rats that bore tumors and also had sterile inflammation. The inflammation was induced by injection of turpentine, which is known to result in exudation of plasma and migration of neutrophils within 24 h (22).

## MATERIALS AND METHODS

### Materials

$^{18}\text{F}$ -FLT was produced by radiofluorination of the 2,3'-anhydro-5'-*O*-(4,4'-dimethoxytrityl)-thymidine precursor, with radiochemical yields of 5%–10%.  $^{18}\text{F}$ -FDG was produced by the Hamacher method (nucleophilic fluorination reaction followed by deprotection). The specific radioactivities of  $^{18}\text{F}$ -FLT and  $^{18}\text{F}$ -FDG were always  $>10$  (usually 50–100) TBq/mmol. Thymidine phosphorylase (from the bacterium *Escherichia coli*) was obtained from Sigma. Matrigel basement membrane matrix was purchased from BD Biosciences. Turpentine came from a local paint shop.

### Animal Model

The experiments were performed by licensed investigators in accordance with the Law on Animal Experiments of The Netherlands. Male Wistar rats (200- to 240-g body weight) were obtained from Harlan. After the rats had been allowed 1 wk of acclimation, C6 glioma cells ( $2 \times 10^6$ , in a 1:1 v/v mixture of Matrigel and Dulbecco's minimal essential medium containing 5% fetal calf serum) were subcutaneously injected into the right shoulder. Matrigel was included to avoid migration of tumor cells to sites other than the place of injection. Ten days later, 0.1 mL of turpentine was intramuscularly injected into the thigh of the left hind leg. After an additional 24 h, the radiopharmaceutical (either  $^{18}\text{F}$ -FDG or  $^{18}\text{F}$ -FLT) was intravenously administered through a tail vein.

### Phosphorylase Pretreatment

To reduce the serum levels of endogenous thymidine, 5 rats were pretreated with thymidine phosphorylase (1,000–1,500 U/kg of body weight) 45 min before injection of  $^{18}\text{F}$ -FLT. The enzyme was administered by intravenous infusion through a tail vein. Because phosphorylase is supplied in potassium phosphate buffer, a slow rate of infusion was used (less than 50  $\mu\text{L}/\text{min}$ ; total volume, 0.6–1.0 mL) to avoid myocardial arrest. Plasma thymidine was measured using reversed-phase high-performance liquid chromatography (23,24).

### Biodistribution Experiments

Twenty-four hours after the turpentine injection, the rats were anesthetized using (*S*)-ketamine (50 mg/kg intraperitoneally) and medetomidine (0.3 mg/kg intraperitoneally). The animals were kept under anesthesia for the rest of the experiment. A bolus of either  $^{18}\text{F}$ -FLT or  $^{18}\text{F}$ -FDG (0.3 mL containing 30 MBq) was administered by intravenous injection through a lateral tail vein. The rats were sacrificed 120 min after radiotracer injection by extirpation of the heart (under general ketamine/medetomidine anesthesia). Blood was collected, and normal tissues (brain, fat, bone, heart, intestines, kidney, liver, lung, skeletal muscle, pan-

creas, spleen, submandibular salivary gland, and urinary bladder) were excised. Urine was collected, and plasma and a red cell fraction were obtained from blood centrifugation (5 min at 1,000g). The complete tumor was excised and carefully separated from muscle and skin. Inflamed muscle was recognizable by its pale color and could generally be distinguished from the surrounding darker tissue. A relatively small sample including the inflamed region ( $0.71 \pm 0.32$  g) was excised from the affected thigh. All samples were weighed, and the radioactivity was measured using a Compugamma CS 1282 counter (LKB-Wallac), applying a decay correction. The results were expressed as dimensionless standardized uptake values (dpm measured per gram of tissue/dpm injected per gram of body weight). Tissue-to-plasma and tumor-to-muscle concentration ratios of radioactivity were also calculated.

### Histologic Examination of Inflamed Muscle and C6 Tumors

Excised tumors and the inflamed parts of the thigh muscle were fixed in formalin and embedded in paraffin. Sections 5  $\mu\text{m}$  thick were stained with hematoxylin and eosin.

### PET Imaging

Rats anesthetized with ketamine and medetomidine were placed into a positron camera (ECAT 962/HR+, 4.5 mm in full width at half maximum; Siemens) and received a bolus injection of either  $^{18}\text{F}$ -FLT or  $^{18}\text{F}$ -FDG (30 MBq) through a tail vein. Data were acquired from 90 to 150 min. A zoom factor of 1.5 was applied during reconstruction (by filtered backprojection), and the matrix size was  $128 \times 128$ .

### Statistical Analysis

Statistical analysis was performed using the software package Statistix (NH Analytic Software). Differences between the various groups ( $^{18}\text{F}$ -FLT,  $^{18}\text{F}$ -FLT with phosphorylase pretreatment, and  $^{18}\text{F}$ -FDG) were tested for statistical significance using the 2-sided student *t* test for independent samples. *P* values  $< 0.05$  were considered significant.

## RESULTS

### Development of Tumor and Inflammation

The growth rate of C6 tumors in Wistar rats proved to be variable. Tumor mass at radiotracer injection was  $1.61 \pm 0.89$  g (mean  $\pm$  SD; range, 0.41–2.97 g). Turpentine injection resulted in visible swelling of the inflamed thigh after 24 h, although the behavior of the rats during this period was normal. The body weight of the animals during the biodistribution experiments was  $325 \pm 27$  g.

### $^{18}\text{F}$ -FLT Uptake in Untreated Rats

In initial experiments on 3 rats, the radiopharmaceutical  $^{18}\text{F}$ -FLT was administered directly to the animals without any pretreatment. To our surprise, the nucleoside did not accumulate above plasma levels in any organ except bone marrow, small intestine, kidney, and urinary bladder (Table 1). Radioactivity did not accumulate even in the C6 tumors (Table 2). High serum levels of endogenous thymidine may have saturated tissue nucleoside transporters or thymidine kinase 1 and have blocked uptake or trapping of  $^{18}\text{F}$ -FLT. Anthony F. Shields (Karmanos Cancer Institute), Peter S.

**TABLE 1**  
Standardized Uptake Values at 120 Minutes After Injection

Tissue	<sup>18</sup> F-FLT untreated (n = 3)	<sup>18</sup> F-FLT + phosphorylase (n = 5)	<sup>18</sup> F-FDG (n = 5)	Effect of phosphorylase on <sup>18</sup> F-FLT uptake	<sup>18</sup> F-FLT + phosphorylase vs. <sup>18</sup> F-FDG
Cerebellum	0.06 ± 0.01	0.04 ± 0.02	1.23 ± 0.29	NS	<0.001
Cortex	0.05 ± 0.01	0.04 ± 0.02	1.86 ± 0.45	NS	<0.001
Rest of brain	0.06 ± 0.01	0.04 ± 0.02	1.45 ± 0.33	NS	<0.001
Adipose tissue	0.14 ± 0.16	0.03 ± 0.02	0.09 ± 0.04	NS	<0.05
Urinary bladder	0.74 ± 0.49	1.57 ± 0.68	1.65 ± 0.92	NS	NS
Bone	0.19 ± 0.03	1.18 ± 0.67	0.35 ± 0.11	0.06	0.09
Bone marrow	1.04 ± 0.54	6.67 ± 2.53	1.55 ± 0.41	<0.02	<0.05
Heart	0.46 ± 0.20	0.26 ± 0.15	5.84 ± 3.29	NS	<0.02
Large intestine	0.54 ± 0.25	0.55 ± 0.16	1.37 ± 0.32	NS	0.001
Small intestine	1.08 ± 0.45	1.28 ± 0.58	1.10 ± 0.23	NS	NS
Kidney	2.28 ± 0.69	1.19 ± 0.49	1.89 ± 0.43	0.06	<0.05
Liver	0.61 ± 0.28	0.39 ± 0.20	0.51 ± 0.11	NS	NS
Lung	0.46 ± 0.16	0.34 ± 0.19	1.15 ± 0.26	NS	0.0005
Muscle	0.42 ± 0.15	0.29 ± 0.09	0.18 ± 0.06	NS	0.05
Pancreas	0.41 ± 0.21	0.26 ± 0.12	0.32 ± 0.05	NS	NS
Plasma	0.58 ± 0.25	0.31 ± 0.15	0.43 ± 0.17	NS	NS
Red blood cells	0.55 ± 0.21	0.31 ± 0.15	0.31 ± 0.09	NS	NS
Spleen	0.56 ± 0.20	1.16 ± 0.63	1.64 ± 0.42	NS	NS
Submandibularis	0.31 ± 0.11	0.34 ± 0.17	1.18 ± 0.30	NS	<0.001
C6 tumor	0.55 ± 0.06	1.14 ± 0.62	2.34 ± 0.72	NS	<0.05
Inflammation	0.51 ± 0.18	0.37 ± 0.16	0.82 ± 0.14	NS	<0.002
Urine	12.6 ± 2.0	16.3 ± 12.4	9.0 ± 2.0	NS	NS

NS = not statistically significant.

The bone sample contained marrow; thus, bone uptake does not reflect defluorination.

Conti, and James R. Bading (University of Southern California) suggested that we infuse thymidine phosphorylase before injection of <sup>18</sup>F-FLT to circumvent this problem. The next 5 rats were pretreated in this way; the radiolabeled nucleoside was administered 45 min after the start of enzyme infusion. Data on untreated animals were compared with data on the thymidine phosphorylase-pretreated group.

#### <sup>18</sup>F-FLT Uptake After Pretreatment

Pretreatment of animals with thymidine phosphorylase (intravenously, 45 min before administration of the radio-

tracer) did not affect tissue-to-plasma ratios of <sup>18</sup>F-FLT in brain, adipose tissue, urinary bladder, heart, kidney, liver, lung, normal and inflamed skeletal muscle, pancreas, or red blood cells. However, infusion of the enzyme increased the accumulation of <sup>18</sup>F-FLT in bone, bone marrow, and the C6 tumor (Tables 1 and 2). Plasma levels of radioactivity tended to decrease after phosphorylase infusion. Thus, tissue-to-plasma ratios of radioactivity were significantly increased in bone, bone marrow, intestines, tumor, spleen, and submandibular salivary gland (data not shown). Tumor-to-muscle ratios of radioactivity also significantly increased

**TABLE 2**  
Tissue-to-Plasma and Tissue-to-Muscle Ratios Besides Selectivity Index (Tumor vs. Inflammation)

Parameter	<sup>18</sup> F-FLT untreated (n = 3)	<sup>18</sup> F-FLT + phosphorylase (n = 5)	<sup>18</sup> F-FDG (n = 5)	Effect of phosphorylase on <sup>18</sup> F-FLT uptake	FLT + phosphorylase vs. <sup>18</sup> F-FDG
Tumor-to-plasma ratio	1.0 ± 0.4	3.8 ± 1.4	6.1 ± 2.7	<0.05	NS
Tumor-to-muscle ratio	1.4 ± 0.4	3.8 ± 1.3	13.2 ± 3.0	0.05	0.001
Inflammation-to-plasma ratio	0.9 ± 0.1	1.2 ± 0.3	2.1 ± 0.8	NS	<0.05
Inflammation-to-muscle ratio	1.2 ± 0.0	1.3 ± 0.4	4.8 ± 1.2	NS	0.0002
Selectivity index*	1.8 ± 1.7	>10.6†	3.5 ± 1.2		

\*Defined as (tumor uptake – muscle uptake)/(inflammation uptake – muscle uptake), that is, tumor-to-inflammation ratio corrected for background activity.

†SD cannot be given because, in some animals, tracer uptake in inflamed muscle equalled that in contralateral healthy muscle.

after phosphorylase treatment (Table 2). Plasma levels of thymidine were measured in a parallel experiment on a single rat and were found to decrease from 0.15  $\mu\text{g}/\text{mL}$  to undetectable levels after phosphorylase infusion.

#### Biodistribution of $^{18}\text{F}$ -FDG and $^{18}\text{F}$ -FLT

The next 5 animals received  $^{18}\text{F}$ -FDG rather than  $^{18}\text{F}$ -FLT, to compare the biodistribution of the 2 radiopharmaceuticals. The glucose analog  $^{18}\text{F}$ -FDG showed physiologic uptake in heart and brain.  $^{18}\text{F}$ -FDG uptake was higher than  $^{18}\text{F}$ -FLT uptake in C6 tumors, inflamed muscle, brain, adipose tissue, kidney, large intestine, lung, and submandibular salivary gland (Table 1). In contrast,  $^{18}\text{F}$ -FLT accumulated more in bone, bone marrow, and healthy muscle than did  $^{18}\text{F}$ -FDG (Table 1).

#### Selectivity of $^{18}\text{F}$ -FDG and $^{18}\text{F}$ -FLT

$^{18}\text{F}$ -FLT did not accumulate in inflammatory tissue (tissue-to-plasma and tissue-to-muscle ratios were not significantly different from unity). However,  $^{18}\text{F}$ -FDG accumulation was 4.8-fold higher ( $P = 0.0002$ ) in inflamed thigh muscle than in the noninflamed contralateral thigh (Table 2). The selectivity index (tumor-to-inflammatory tissue ratio corrected for uptake in healthy muscle) was  $>10.6$  for  $^{18}\text{F}$ -FLT and 3.5 for  $^{18}\text{F}$ -FDG (Table 2).

Tumor-to-plasma ratios of  $^{18}\text{F}$ -FLT and  $^{18}\text{F}$ -FDG were not significantly different, but tumor-to-muscle ratios of  $^{18}\text{F}$ -FDG were significantly higher ( $P = 0.001$ ) than those of  $^{18}\text{F}$ -FLT (Table 2).

#### Histology of Inflamed Muscle and C6 Tumors

Histologic examination of the muscle specimens excised 24 h after turpentine injection showed an acute inflammatory reaction. Massive infiltration of neutrophils was seen in and between partially necrotic muscle fibers—the picture of acute myositis (Fig. 1). In the border of the inflammatory infiltrate, macrophages and few fibroblasts could be discerned.

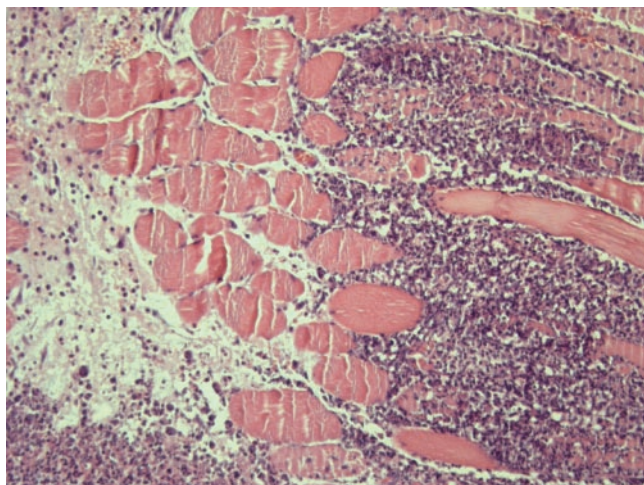


**FIGURE 1.** Microscopic image of a specimen of inflamed rat muscle, 24 h after injection of turpentine (hematoxylin and eosin,  $\times 400$ ).

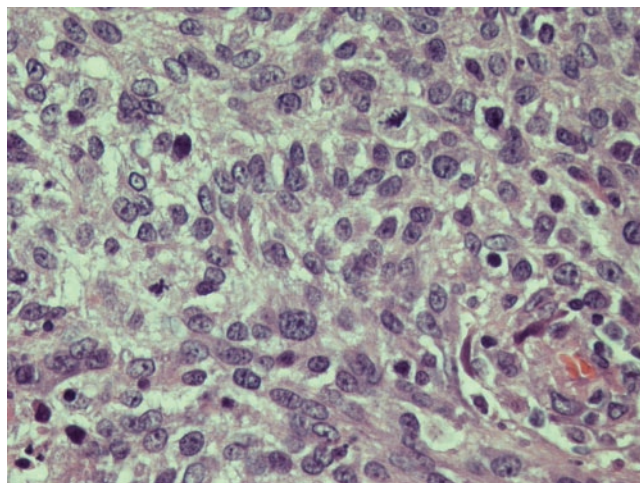


**FIGURE 2.** Microscopic image of a specimen of rat tumor, 11 d after inoculation of C6 cells (hematoxylin and eosin,  $\times 400$ ).

Histologic examination of the excised C6 tumors showed a malignant mesenchymal tumor (Fig. 2). Spindled tumor cells with pleomorphic, hyperchromatic nuclei were arranged in short bundles. Many mitoses were found (range, 25–40 per  $2\text{ mm}^2$ ). Small areas of tumor necrosis were seen, composing less than 10% of the total tumor volume.

#### PET Images

PET images, obtained with the 2 tracers, of tumor- and inflammation-bearing rats are shown in Figure 3. The head of each animal is on the right, and the rats are seen from below. Both  $^{18}\text{F}$ -FLT and  $^{18}\text{F}$ -FDG clearly revealed the C6 tumor in the right shoulder.  $^{18}\text{F}$ -FDG showed high, physiologic uptake in the brain, in contrast to  $^{18}\text{F}$ -FLT. The inflammation in the left hind leg was revealed with  $^{18}\text{F}$ -FDG but not with  $^{18}\text{F}$ -FLT.

#### DISCUSSION

This study confirmed that the standardized uptake value of  $^{18}\text{F}$ -FLT in inflammatory tissue is lower than that of  $^{18}\text{F}$ -FDG (Table 1; Fig. 3). Although the tumor uptake of  $^{18}\text{F}$ -FLT is also considerably lower than that of  $^{18}\text{F}$ -FDG

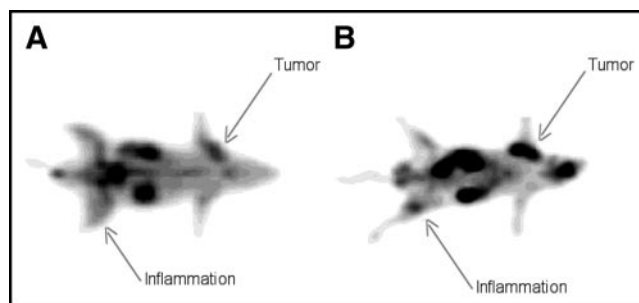


**FIGURE 3.** PET images obtained 110–130 min after injection of 30 MBq of  $^{18}\text{F}$ -FLT (A) and  $^{18}\text{F}$ -FDG (B) into rats.  $^{18}\text{F}$ -FLT reveals only the tumor, whereas both tumor and inflammation are visible after injection of  $^{18}\text{F}$ -FDG.

(Table 1), the selectivity of  $^{18}\text{F}$ -FLT for tumor versus inflammation is nevertheless higher than that of glucose analog: 10.6- versus 3.5-fold at 120 min after injection, when the data are corrected for background activity (Table 2). Thus, the hypothesis that  $^{18}\text{F}$ -FLT has a higher tumor specificity was confirmed in our animal model.

Standardized uptake values of  $^{18}\text{F}$ -FDG in C6 tumors were 2-fold higher than those of  $^{18}\text{F}$ -FLT. Tumor-to-muscle ratios of  $^{18}\text{F}$ -FDG ( $13.2 \pm 3.0$ ) were clearly superior to those of  $^{18}\text{F}$ -FLT ( $3.8 \pm 1.3$ ). These results are in accordance with clinical data from  $^{18}\text{F}$ -FDG and  $^{18}\text{F}$ -FLT PET scans, in which colorectal cancers have been found to display a 2-fold higher standardized uptake value of  $^{18}\text{F}$ -FDG than of  $^{18}\text{F}$ -FLT (25).

However,  $^{18}\text{F}$ -FDG showed relatively poor selectivity for distinguishing tumor from inflammatory tissue. The inflamed thigh was clearly visualized in a PET image (Fig. 3). Tissue uptake of  $^{18}\text{F}$ -FDG was 4.8-fold greater in inflamed muscle than in the contralateral healthy leg, and the selectivity index of  $^{18}\text{F}$ -FDG for tumor versus inflammation was 3.5 (Table 2). Because only part of the volume of the inflamed muscle samples consisted of neutrophils and macrophages,  $^{18}\text{F}$ -FDG uptake in these inflammatory cells may have been >10-fold greater than in normal muscle cells.

$^{18}\text{F}$ -FLT showed better tumor selectivity in our model than did  $^{18}\text{F}$ -FDG. In a PET image (Fig. 3), the inflamed thigh showed tracer uptake similar to that in the contralateral healthy thigh. Biodistribution studies indicated that accumulation of  $^{18}\text{F}$ -FLT in inflamed muscle was not significantly different from that in noninflamed tissue of the contralateral thigh (ratio,  $1.3 \pm 0.4$ ; Table 2). The selectivity index of  $^{18}\text{F}$ -FLT for tumor versus inflammation was 10.6 or greater (Table 2).

In Wistar rats, the glucose analog showed a biodistribution that was expected on the basis of clinical  $^{18}\text{F}$ -FDG PET scans, that is, high and physiologic uptake in brain and heart, besides renal excretion and accumulation in urine (Table 1). In contrast to  $^{18}\text{F}$ -FDG,  $^{18}\text{F}$ -FLT accumulated mainly in bone marrow (Table 1). Low levels of radioactivity in the brain were probably due to the slow transportation of  $^{18}\text{F}$ -FLT across the blood-brain barrier or to the low activity of thymidine kinase in the brain.

The data presented in the tables indicate that endogenous thymidine can strongly affect in vivo uptake of  $^{18}\text{F}$ -FLT. Low tissue uptake of  $^{18}\text{F}$ -FLT in untreated rats is probably a consequence of high levels of endogenous thymidine in rodent serum (26), since previous infusion of thymidine phosphorylase significantly increased uptake of the radiolabeled nucleoside in target organs (Table 1). Thymidine may compete with  $^{18}\text{F}$ -FLT for the active site of nucleoside carriers in cell membranes (27) and also for the active site of the trapping enzyme, thymidine kinase 1. The affinity of human thymidine kinase 1 for thymidine has been reported to be 4-fold higher ( $0.5 \mu\text{mol/L}$ ) than is the affinity for  $^{18}\text{F}$ -FLT ( $2.1 \mu\text{mol/L}$ ) (21).

Apparently, substantial plasma concentrations of endogenous thymidine can suppress  $^{18}\text{F}$ -FLT uptake in most tissues (Table 1). In contrast to rats, humans have much (9- to 16-fold) lower levels of serum thymidine ( $0.01$ – $0.02 \mu\text{g/mL}$  vs.  $0.15$ – $0.27 \mu\text{g/mL}$ ) (26). Therefore,  $^{18}\text{F}$ -FLT PET scans of cancer patients show adequate image contrast (19,20,25,28,29).

After infusion of a thymidine-degrading enzyme, physiologic accumulation of  $^{18}\text{F}$ -FLT to levels greater than those in plasma was observed in C6 tumors, bone, bone marrow, large and small intestine, and spleen (Table 1). Many of these organs contain rapidly dividing tissue (malignant cells in the tumor, bone marrow in the skeleton, mucosa in the intestines). Thus, in pretreated rats,  $^{18}\text{F}$ -FLT behaved as a tracer of cellular proliferation. This finding is in accordance with reports from the literature suggesting a significant correlation between standardized uptake values of  $^{18}\text{F}$ -FLT and proliferative activity of various lesions (28,30,31). In vitro studies have shown that  $^{18}\text{F}$ -FLT uptake is related to thymidine kinase-1 activity and the percentage of cells in S-phase (16,17).  $^{18}\text{F}$ -FDG accumulated in the same rapidly dividing tissues as did  $^{18}\text{F}$ -FLT (Table 2) and showed even higher standardized uptake values in tumor and large intestine.

## CONCLUSION

In our animal model,  $^{18}\text{F}$ -FLT revealed only tumor, whereas  $^{18}\text{F}$ -FDG delineated both tumor and inflammation. On the basis of these animal data,  $^{18}\text{F}$ -FLT scans of oncologic patients can be expected to show more false-negative findings (because of lower tumor uptake) and fewer false-positive findings (because of negligible accumulation in granulocytes) than do whole-body  $^{18}\text{F}$ -FDG scans.

## ACKNOWLEDGMENTS

We thank Dr. Tony Lahoutte (Free University of Brussels) for valuable information on the turpentine inflammation model; Drs. Anthony F. Shields (Karmanos Cancer Institute), Peter S. Conti, and James R. Bading (University of Southern California) for their suggestion that we lower endogenous thymidine levels by intravenous infusion of thymidine phosphorylase; and Biotechnicians Hans Bartels, Ar Jansen, and Arie Nijmeijer (Central Animal Laboratory, University of Groningen) for expert technical assistance. This work was supported by the Dutch Cancer Society (Koningin Wilhelmina Fonds, KWF, grant 2000-2299)

## REFERENCES

1. Lorenzen J, de Wit M, Buchert R, Igel B, Bohuslavizki KH. Granulationsgewebe: pitfall in der therapiekontrolle mit F-18-FDG-PET nach chemotherapie. *Nuklearmedizin*. 1999;38:333-336.
2. Shreve PD, Anzai Y, Wahl RL, Shreve PD, Anzai Y, Wahl RL. Pitfalls in oncologic diagnosis with FDG PET imaging: physiologic and benign variants. *Radiographics*. 1999;19:61-77.
3. Strauss LG. Fluorine-18 deoxyglucose and false-positive results: a major problem in the diagnostics of oncological patients. *Eur J Nucl Med*. 1996;23:1409-1415.
4. Zhuang H, Cunnane ME, Ghesani NV, Mozley PD, Alavi A. Chest tube insertion

- as a potential source of false-positive FDG-positron emission tomographic results. *Clin Nucl Med.* 2002;27:285–286.
5. Kerrou K, Montravers F, Grahek D, et al. [<sup>18</sup>F]-FDG uptake in soft tissue dermatome prior to herpes zoster eruption: an unusual pitfall. *Ann Nucl Med.* 2001;15:455–458.
  6. Shreve PD. Focal fluorine-18 fluorodeoxyglucose accumulation in inflammatory pancreatic disease. *Eur J Nucl Med.* 1998;25:259–264.
  7. Kaim AH, Weber B, Kurrer MO, Gottschalk J, von Schulthess GK, Buck A. Autoradiographic quantification of <sup>18</sup>F-FDG uptake in experimental soft-tissue abscesses in rats. *Radiology.* 2002;223:446–451.
  8. Kubota R, Kubota K, Yamada S, Tada M, Ido T, Tamahashi N. Microautoradiographic study for the differentiation of intratumoral macrophages, granulation tissues and cancer cells by the dynamics of fluorine-18-fluorodeoxyglucose uptake. *J Nucl Med.* 1994;35:104–112.
  9. Kubota R, Yamada S, Kubota K, Ishiwata K, Tamahashi N, Ido T. Intratumoral distribution of fluorine-18-fluorodeoxyglucose in vivo: high accumulation in macrophages and granulation tissues studied by microautoradiography. *J Nucl Med.* 1992;33:1972–1980.
  10. Sugawara Y, Gutowski TD, Fisher SJ, Brown RS, Wahl RL. Uptake of positron emission tomography tracers in experimental bacterial infections: a comparative biodistribution study of radiolabeled FDG, thymidine, L-methionine, <sup>67</sup>Ga-citrate, and <sup>125</sup>I-HSA. *Eur J Nucl Med.* 1999;26:333–341.
  11. Wahl RL, Fisher SJ. A comparison of FDG, L-methionine and thymidine accumulation into experimental infections and reactive lymph nodes [abstract]. *J Nucl Med.* 1993;34(suppl):104P
  12. Mankoff DA, Shields AF, Link JM, et al. Kinetic analysis of 2-[<sup>11</sup>C]thymidine PET imaging studies: validation studies. *J Nucl Med.* 1999;40:614–624.
  13. Krohn KA, Mankoff DA, Eary JF. Imaging cellular proliferation as a measure of response to therapy. *J Clin Pharmacol.* 2001;July(suppl):96S–103S.
  14. Mankoff DA, Shields AF, Graham MM, Link JM, Eary JF, Krohn KA. Kinetic analysis of 2-[carbon-11]thymidine PET imaging studies: compartmental model and mathematical analysis. *J Nucl Med.* 1998;39:1043–1055.
  15. Shields AF, Grierson JR, Kozawa SM, Zheng M. Development of labeled thymidine analogs for imaging tumor proliferation. *Nucl Med Biol.* 1996;23:17–22.
  16. Rasey JS, Grierson JR, Wiens LW, Kolb PD, Schwartz JL. Validation of FLT uptake as a measure of thymidine kinase-1 activity in A549 carcinoma cells. *J Nucl Med.* 2002;43:1210–1217.
  17. Toyohara J, Waki A, Takamatsu S, Yonekura Y, Magata Y, Fujibayashi Y. Basis of FLT as a cell proliferation marker: comparative uptake studies with [<sup>3</sup>H]thymidine and [<sup>3</sup>H]arabinothymidine, and cell-analysis in 22 asynchronously growing tumor cell lines. *Nucl Med Biol.* 2002;29:281–287.
  18. Seitz U, Wagner M, Neumaier B, et al. Evaluation of pyrimidine metabolising enzymes and in vitro uptake of 3'-[(18)F]fluoro-3'-deoxythymidine ([<sup>18</sup>F]FLT) in pancreatic cancer cell lines. *Eur J Nucl Med Mol Imaging.* 2002;29:1174–1181.
  19. Wagner M, Seitz U, Buck A, et al. 3'-[(18)F]fluoro-3'-deoxythymidine ([<sup>18</sup>F]-FLT) as positron emission tomography tracer for imaging proliferation in a murine B-cell lymphoma model and in the human disease. *Cancer Res.* 2003;63:2681–2687.
  20. Shields AF, Grierson JR, Dohmen BM, et al. Imaging proliferation in vivo with [F-18]FLT and positron emission tomography. *Nat Med.* 1998;4:1334–1336.
  21. Munch-Petersen B, Cloos L, Tyrsted G, Eriksson S. Diverging substrate specificity of pure human thymidine kinases 1 and 2 against antiviral dideoxynucleosides. *J Biol Chem.* 1991;266:9032–9038.
  22. Yamada S, Kubota K, Kubota R, Ido T, Tamahashi N. High accumulation of fluorine-18-fluorodeoxyglucose in turpentine-induced inflammatory tissue. *J Nucl Med.* 1995;36:1301–1306.
  23. Van Waarde A, Avison MJ, Thulin G, Gaudio KM, Shulman RG, Siegel NJ. Role of nucleoside uptake in renal postischemic ATP synthesis. *Am J Physiol.* 1992; 262:F1092–F1099.
  24. Olivares J, Verdys M. Isocratic high-performance liquid chromatographic method for studying the metabolism of blood plasma pyrimidine nucleosides and bases: concentration and radioactivity measurements. *J Chromatogr.* 1988;434:111–121.
  25. Francis DL, Visvikis D, Costa DC, et al. Potential impact of [(18)F]3'-deoxy-3'-fluorothymidine versus [(18)F]fluoro-2-deoxy-d-glucose in positron emission tomography for colorectal cancer. *Eur J Nucl Med Mol Imaging.* 2003;30:988–994.
  26. Nottebrock H, Then R. Thymidine concentrations in serum and urine of different animal species and man. *Biochem Pharmacol.* 1977;26:2175–2179.
  27. Kong XB, Zhu QY, Vidal PM, et al. Comparisons of anti-human immunodeficiency virus activities, cellular transport, and plasma and intracellular pharmacokinetics of 3'-fluoro-3'-deoxythymidine and 3'-azido-3'-deoxythymidine. *Antimicrob Agents Chemother.* 1992;36:808–818.
  28. Buck AK, Schirrmeister H, Hetzel M, et al. 3-deoxy-3'-[(18)F]fluorothymidine-positron emission tomography for noninvasive assessment of proliferation in pulmonary nodules. *Cancer Res.* 2002;62:3331–3334.
  29. Vesselle H, Grierson J, Muzi M, et al. In vivo validation of 3'-deoxy-3'-[(18)F]fluorothymidine ([<sup>18</sup>F]FLT) as a proliferation imaging tracer in humans: correlation of [<sup>18</sup>F]FLT uptake by positron emission tomography with Ki-67 immunohistochemistry and flow cytometry in human lung tumors. *Clin Cancer Res.* 2002;8:3315–3323.
  30. Barthel H, Cleij MC, Collingridge DR, et al. 3'-deoxy-3'-[(18)F]fluorothymidine as a new marker for monitoring tumor response to antiproliferative therapy in vivo with positron emission tomography. *Cancer Res.* 2003;63:3791–3798.
  31. Dittmann H, Dohmen BM, Kehlbach R, et al. Early changes in [(18)F]FLT uptake after chemotherapy: an experimental study. *Eur J Nucl Med Mol Imaging.* 2002;29:1462–1469.